Astron. Astrophys. 334, 99–109 (1998)

ASTRONOMY AND ASTROPHYSICS

# Evolution of the colour-magnitude relation of early-type galaxies in distant clusters

**Tadayuki Kodama**[1,2], **Nobuo Arimoto**[2,4], **Amy J. Barger**[1,3], **and Alfonso Aragón-Salamanca**[1]

[1] Institute of Astronomy, University of Cambridge, Madingley Road, Cambridge CB3 0HA, UK (kodama@ast.cam.ac.uk)
[2] Institute of Astronomy, University of Tokyo, Mitaka, Tokyo 181, Japan
[3] Institute for Astronomy, University of Hawaii, 2680 Woodlawn Drive, Honolulu, Hawaii 96822, USA
[4] Observatoire de Paris, Section de Meudon, DAEC, F-92195 Meudon Principle Cedex, France

Received 21 November 1997 / Accepted 17 February 1998

**Abstract.** We present a thorough quantitative analysis of the evolution of the colour-magnitude relation for early-type galaxies in 17 distant clusters with redshifts $0.31 < z < 1.27$ using the Kodama & Arimoto (1997) evolutionary model for elliptical galaxies. The model is calibrated to reproduce the colour-magnitude relation for Coma ellipticals at $z \sim 0$ and gives the evolution of the slope and zero-point as a function of redshift. We find no significant differences between the colour-magnitude relations of the clusters in our sample. The slopes can be reproduced by a single model sequence in which all elliptical galaxies are assumed to be equally old (the maximum age difference allowed for the brightest 3 magnitudes is only 1 Gyr) and to have mean stellar metallicities which vary as a function of galaxy luminosity. The zero-points of the colour-magnitude relations constrain the epoch of major star formation in early-type galaxies to $z_f > 2$–4. This study provides two important constraints for any model of the formation of rich clusters: the uniformity of the ages of the stellar populations in the early-type galaxies and the universality of the metallicity sequence of these galaxies as a function of galaxy mass.

**Key words:** galaxies: active – galaxies: elliptical and lenticular, cD – galaxies: evolution – galaxies: formation – galaxies: photometry – galaxies: stellar content

## 1. Introduction

Visvanathan & Sandage (1977) first noted from their data on 9 nearby clusters that the more luminous early-type galaxies tended to have redder colours. Bower, Lucey, & Ellis (1992; hereafter BLE92) later studied this *colour-magnitude* (*C-M*) relation in detail using high precision photometry of early-type galaxies in the Virgo and Coma clusters and found very little scatter about the mean *C-M* relation. Thus, there appeared to be a marked homogeneity in the present-day early-type cluster galaxy population. Recently, Kodama & Arimoto (1997; hereafter KA97) compared the predictions of their evolutionary models of elliptical galaxies with the *C-M* diagrams for early-type galaxies in two distant clusters, Abell 2390 at $z = 0.228$ and Abell 851 at $z = 0.407$, and showed that the origin of the *C-M* relation was primarily due to the mean stellar metallicity of the early-types being a function of total magnitude. In this paper we present a more thorough study of the evolution of the *C-M* relation by using 17 clusters at cosmological distances to detect the colour evolution of cluster early-type galaxies directly and then comparing the results with the models. This will enable us to put even stronger constraints on the formation of early-type galaxies in clusters.

The photometric evolution of early-type galaxies in $z < 1$ clusters was previously examined by several authors (e.g., Ellis et al. 1985; Couch, Shanks & Pence 1985; Aragón-Salamanca et al. 1993). Aragón-Salamanca et al. (1993) traced the evolution of the 'red envelope' from the optical-near-infrared colour distribution of galaxies in 10 clusters with redshifts $0.5 < z < 0.9$ and concluded that the detected evolution was consistent with the passive ageing of stellar populations formed before $z \simeq 2$. A potential problem with these studies is that the early-type galaxies had to be selected by their spectral energy distributions and colours, thereby increasing the possibility of contamination from other galaxy types. The advent of the Hubble Space Telescope *(HST)*, with its spectacular high-resolution images, has made the morphological classification of distant galaxies possible. Furthermore, thanks to the *HST*, large ground-based telescopes, and the high quality of astronomical detectors, much fainter limiting magnitudes can now be reached. An additional advantage of *HST* photometry comes from the reduction of the sky background at longer wavelengths compared to that achieved with ground-based observations (e.g. the background in space is 8 times fainter in the $I$-band), thereby reducing the photometric errors at faint limits significantly (Ellis et al. 1997; hereafter E97). These improvements now make it possible to examine the evolution of early-type galaxies over a much wider luminosity and redshift range.

The *C-M* relation is a powerful tool for quantifying the colour evolution of early-type galaxies as a function of redshift since it can be observed up to very high redshifts. Dickinson (1996) showed that the *C-M* relation is already recognizable at

*Send offprint requests to*: T. Kodama

$z \simeq 1.2$. The zero-point of the *C-M* relation at high redshift provides direct information on the properties of early-type galaxies in general. On the other hand, the slope of the *C-M* relation has information on differential properties of early-type galaxies as a function of luminosity or galaxy size.

Stanford, Eisenhardt, & Dickinson (1995; 1998, hereafter SED98) presented *C-M* relations for morphologically selected early-type galaxies in 19 clusters out to $z = 0.9$. When they compared their optical-near-infrared *C-M* relations to that of Coma, they found no significant change in either the slope or the scatter as a function of redshift. They did, however, observe a progressive blueing with redshift of the average colour in a manner consistent with the passive evolution of an old stellar population formed in a burst at an early cosmic epoch.

E97 also analyzed the *C-M* relations of three distant clusters at $z \simeq 0.54$ (Cl 0016+16, Cl 0054−27, Cl 0412−65), in this case using *HST* photometry. They found that the dispersion about the relations was quite small even in such distant clusters, thereby requiring a high formation redshift for the stars in early-type galaxies, such as $z \simeq 3$. E97 also did not detect a significant change in the slopes of the relations in the rest-frame $U-V$ when compared with Coma. The zero-points show modest colour evolution in agreement with earlier studies (Ellis et al. 1985; Couch et al. 1985; Aragón-Salamanca et al. 1993). All of these results support a formation picture of early-type galaxies in which the bulk of the star formation is completed at high redshift with little star formation occurring in the recent past. Thus, the *C-M* relation originates at high redshift as a metallicity effect.

Recently, however, Kauffmann & Charlot (1997) have argued that the *C-M* relation can alternatively be interpreted in the context of the hierarchical models of galaxy formation once chemical enrichment is taken into account. In their analysis, the slope of the *C-M* relation is maintained because large ellipticals form primarily from large metal-rich progenitors. They find that it remains nearly constant up to $z \simeq 1$. Furthermore, they are able to explain the tightness of the *C-M* relation, despite frequent galaxy merging, by suggesting that we are biasing ourselves to the selection of only old galaxies by studying rich clusters at high redshift. According to their models, these objects are not the progenitors of present-day clusters. It is not yet clear whether this type of model can give an universal *C-M* relation for different clusters, since merging histories are likely to have varied from cluster to cluster.

Our motivations to conduct further analyses on the evolution of the *C-M* relation for cluster early-type galaxies are twofold: (1) to investigate the universality of the *C-M* relation in clusters and (2) to put stronger constraints on the formation of early-type galaxies by using the more realistic elliptical galaxy model of KA97, which takes into account chemical evolution, rather than an ad-hoc single burst model with fixed metallicity ($Z_\odot$) adopted by most of the previous analyses. KA97 have constructed an evolutionary model of elliptical galaxies which uses a population synthesis technique based on a monolithic collapse picture of galaxy formation. The marked advantage of the KA97 model is that it allows us to analyze both the slope of the *C-M* relation and the zero-point, since it includes the effects of metallicity. Moreover, since the model is calibrated with the empirical colours of ellipticals in Coma, it can be directly and reliably compared to the observational data in distant clusters.

In this paper, we investigate the evolution of the *C-M* relation of 17 distant clusters using the KA97 evolutionary models. We have accumulated the photometric data from the literature, most of which were obtained with the *HST* and large, ground-based telescopes ($\sim$ 2–4 m). Although some of the *HST* data suffer from zero-point uncertainties due to the paucity of observed standard stars (see below), their random photometric errors are very small down to $\sim 3$ mag from the brightest end of the *C-M* relation (typically $0.01 - 0.07$ mag). Thus, we are able to conduct a reliable analysis of, for example, the slope of the *C-M* relation based on the relative photometry within each cluster. To constrain the formation epoch of early-type galaxies in clusters, we also conduct a zero-point analysis using only those clusters which have been calibrated with ground-based photometry or those which are at sufficiently high redshift that the evolutionary changes are large enough to put some constraint on the formation epoch, despite relatively large zero-point uncertainties.

The cosmological parameters we have chosen to use throughout this paper are $H_0 = 50\,\mathrm{km\,s^{-1}\,Mpc^{-1}}$ ($h \equiv H_0/100 = 0.5$) and $q_0 = 0.5$, without a lambda term, unless otherwise stated. The structure of this paper is as follows. In Sect. 2 we compile the observational data and define the observed *C-M* relation for each cluster. In Sect. 3 we give a brief description of the evolutionary models of KA97. We compare the models and the observations in Sect. 4, and in Sect. 5 we give a discussion of the results and our conclusions.

## 2. Data

### *2.1. Sources*

Our dataset for this analysis consists of 16 clusters with redshifts between $z = 0.31$ and $z = 1.206$ from various sources, all of which have been imaged with the Wide Field and Planetary Camera 2 (WFPC2) on the *HST*. Here we denote the *HST* magnitudes in the WFPC2 filters F555W, F702W, and F814W by $V_{555}$, $R_{702}$, and $I_{814}$, respectively. We have included one additional cluster, CIG J0848+4453 at $z = 1.273$, which was not observed with the *HST*, but being at the highest redshift, it can place useful constraints.

In this paper we construct optical-$K$ *C-M* relations for six clusters, namely AC 103, AC 114, AC 118, Cl 0024+16, Cl 0016+16, and 3C 324. For the remaining clusters we adopt *C-M* relations given in the literature: (1) ground-based optical$-K$ colour versus total $K$ magnitude for 11 clusters between $z = 0.461$ and 0.895 from SED98; (2) *HST* optical-optical ($V_{555} - I_{814}$) colour versus total $I_{814}$ magnitude for 3 clusters at $z \sim 0.55$ from E97.

A complete list of the clusters used in this study are given in Table 1, along with a summary of their relevant properties. Columns 1–4 list the cluster name, redshift, total number of isolated, morphologically classified spheroidals within the magnitude limit, and the total number of spheroidals excluded from the

**Table 1.** Cluster samples and the regression lines for the *C-M* relations.

| cluster | $z$ | $N_1$ | $N_2$ | d.a. | colour | mag | $M_0$ | $A$ | $B$ | ref |
|---|---|---|---|---|---|---|---|---|---|---|
| AC 103 | 0.31 | 25 | 4 | 28 | $R_{702}-K$ | $K_{\rm rest}$ | $-25$ | $3.23\pm0.04$ | $-0.047\pm0.065$ | 1 |
| | | 25 | 4 | 28 | $I-K$ | $K_{\rm rest}$ | $-25$ | $2.70\pm0.04$ | $-0.054\pm0.052$ | 1 |
| AC 114 | 0.31 | 30 | 4 | 28 | $R_{702}-K$ | $K_{\rm rest}$ | $-25$ | $3.13\pm0.03$ | $-0.027\pm0.032$ | 1 |
| | | 30 | 4 | 28 | $I-K$ | $K_{\rm rest}$ | $-25$ | $3.33\pm0.02$ | $-0.083\pm0.024$ | 1 |
| AC 118 | 0.31 | 35 | 3 | 28 | $R_{702}-K$ | $K_{\rm rest}$ | $-25$ | $3.04\pm0.03$ | $-0.115\pm0.027$ | 1 |
| | | 35 | 4 | 28 | $I-K$ | $K_{\rm rest}$ | $-25$ | $2.77\pm0.02$ | $-0.134\pm0.028$ | 1 |
| Cl $0024+16$ | 0.39 | 28 | 0 | 32 | $I_{814}-K$ | $K_{\rm rest}$ | $-25$ | $3.08\pm0.02$ | $-0.091\pm0.028$ | 1 |
| 3C 295 | 0.461 | 25 | — | 24 | $V-K$ | $K^T$ | $-25.5$ | $4.98\pm0.07$ | $-0.09\pm0.04$ | 3 |
| Cl $0412-65$ | 0.510 | 29 | 9 | 10 | $V_{555}-I_{814}$ | $I^T_{814}$ | $-22$ | $2.32\pm0.03$ | $-0.091\pm0.029$ | 2 |
| | | 29 | — | 24 | $V-K$ | $K^T$ | $-25.5$ | $5.30\pm0.06$ | $-0.09\pm0.04$ | 3 |
| GHO $1601+4253$ | 0.539 | 42 | — | 26 | $V-K$ | $K^T$ | $-25.5$ | $5.33\pm0.06$ | $-0.09\pm0.04$ | 3 |
| MS $0451.6-0306$ | 0.539 | 51 | — | 26 | $V-K$ | $K^T$ | $-25.5$ | $5.24\pm0.06$ | $-0.12\pm0.03$ | 3 |
| Cl $0016+16$ | 0.546 | 25 | 4 | 36 | $I_{814}-K$ | $K_{\rm rest}$ | $-25$ | $2.87\pm0.02$ | $-0.046\pm0.031$ | 1 |
| | | 106 | 15 | 10 | $V_{555}-I_{814}$ | $I^T_{814}$ | $-22$ | $2.38\pm0.01$ | $-0.067\pm0.010$ | 2 |
| | | 65 | — | 26 | $V-K$ | $K^T$ | $-25.5$ | $5.20\pm0.07$ | $-0.08\pm0.02$ | 3 |
| Cl $0054-27$ | 0.563 | 36 | 6 | 10 | $V_{555}-I_{814}$ | $I^T_{814}$ | $-22$ | $2.28\pm0.02$ | $-0.090\pm0.015$ | 2 |
| | | 38 | — | 26 | $V-K$ | $K^T$ | $-25.5$ | $5.34\pm0.06$ | $-0.14\pm0.03$ | 3 |
| 3C 220.1 | 0.620 | 22 | — | 27 | $V-K$ | $K^T$ | $-25.5$ | $5.62\pm0.07$ | $-0.13\pm0.04$ | 3 |
| 3C 34 | 0.689 | 19 | — | 24 | $V-K$ | $K^T$ | $-25.5$ | $5.78\pm0.06$ | $-0.11\pm0.04$ | 3 |
| GHO $1322+3027$ | 0.751 | 23 | — | 24 | $R-K$ | $K^T$ | $-26$ | $4.56\pm0.06$ | $-0.07\pm0.03$ | 3 |
| MS $1054.5-032$ | 0.828 | 71 | — | 22 | $R-K$ | $K^T$ | $-26$ | $4.85\pm0.06$ | $-0.11\pm0.02$ | 3 |
| GHO $1603+4313$ | 0.895 | 23 | — | 21 | $R-K$ | $K^T$ | $-26$ | $5.01\pm0.06$ | $-0.13\pm0.03$ | 3 |
| 3C 324 | 1.206 | 13 | 1 | — | $R-K$ | $K$ | $-26$ | $5.84\pm0.05$ | $-0.099\pm0.065$ | 4 |
| CIG J$0848+4453$ | 1.273 | 6 | 0 | 17 | $R-K$ | $K$ | | $^\dagger5.92\pm0.25$ | | 5 |

$N_1$ — total number of ellipticals, $N_2$ — number of excluded objects, d.a. — diameter aperture in kpc,
$M_0$ — absolute magnitude of C-M zero-point, $A$ and $B$ — coefficients of C-M relation ($^\dagger$ shows average colour). ,
refs. — 1: Barger et al. (1997), 2: Ellis et al. (1997), 3: Stanford et al. (1998), 4: Dickinson (1996), 5: Stanford et al. (1997)

analysis because of their anomalous colours (see discussion below). Column 5 gives the adopted apertures in which the colour and magnitude measurements were made, in units of kpc. Note that the $I_{814}$ magnitudes from E97 and the $K$ magnitudes from SED98 are total magnitudes, as indicated by the subscript $T$. The colours and magnitudes used to define the *C-M* relation for each cluster are given in Columns 6 and 7, respectively. The subscript 'rest' means the magnitude is in the rest frame; all others are given in the frame of the observer. Column 8 lists the absolute magnitude, $M_0$, which defines the zero-point of the *C-M* relation for each cluster, and Columns 9 and 10 give the corresponding *C-M* relation regression coefficients (see Sect. 2.2). Finally, Column 11 lists the references for the data.

### *2.2. Colour-magnitude relations*

For five clusters, AC 103, AC 114, AC 118, Cl 0024+16, and Cl 0016+16, we have used the morphological classifications given in Couch et al. (1997) and Smail et al. (1997) to select a sample of *isolated* (i.e. uncontaminated by nearby objects which would distort the colours) early-type (E, E/S0, or S0) galaxies from the cluster cores.

The reliability of the morphological selection of spheroidal galaxies in clusters at $z\sim0.55$ was examined in detail by E97. Visual classifications were found to be robust to $I_{814}\leq21.0$, but over the interval $I_{814}=21.0-22.0$ the distinction between the early-type classes became increasingly uncertain. Principally for this reason we have decided not to attempt to separately analyze the elliptical and S0 galaxy populations. This will also increase our sample size and hence improve the statistics. Since E97 found no evidence for a distinction between the *C-M* relations for the E and S0 populations, our decision to combine these morphological types should not affect the results of our analysis. Moreover, Dressler et al. (1997) point out that the number fraction of S0 galaxies in clusters are rapidly decreasing as a function of redshift, and above redshift 0.6 or so, S0 galaxies could almost disappear.

To construct our *C-M* diagrams, we use ground-based $I$ and $K$-band data for AC 103, AC 114 and AC 118 from Barger et al. (1996) and ground-based $K$-band data for Cl 0024+16 and Cl 0016+16 from Barger et al. (1997). We also use existing *HST* optical data in either the $R_{702}$ or $I_{814}$ bands. We selected magnitude limits such that the samples would contain approximately the brightest 3 mag in the $K$ band. The actual absolute magnitude limits depend on the depth of the $K$-band images and the redshift of the clusters, but they all lie between $M_K=-23$ and $-24$. We present $K$-band magnitudes as absolute magnitudes in the rest frame for the clusters in our sub-sample. The $k$-corrections are determined from a typical spectral energy distribution (SED) of giant elliptical galaxies (Aragón-Salamamca et al. 1993). The SED changes along the *C-M* relation and hence the correct amount of $k$-correction is

varied towards fainter galaxies, however this effect is negligible. Acording to the model SEDs, the difference in the $k$-correction across the *C-M* relation is about only 0.1 magnitude at most, and the effect on both the *C-M* slopes and the zero-points are negligible in our analysis. The seeing corrections are made from an estimate of how much light falls outside the adopted aperture due to scattering, and the Galactic extinction corrections are determined from the $E(B-V)$ values toward the clusters as estimated by the HI intensity (Burstein & Heiles 1984). We adopt $E(B-V)=0.04$ for AC 114, 0.05 for AC 103, 0.055 for AC 118, and 0.03 for Cl 0024+16 and Cl 0016+16.

For the high redshift cluster 3C 324 at $z=1.206$, we adopted $R-K$ colours and $K$ magnitudes of 13 galaxies in the 'red finger' with $K<19$ mag (Dickinson 1996). These galaxies have been confirmed to be early-types from *HST* WFPC2 imaging.

Fig. 1 shows the *C-M* diagrams for the early-type galaxies in our sub-sample of six clusters above. The open circles with filled dots represent the spectroscopically confirmed members. The crosses indicate the objects whose colours place them clearly outside the *C-M* relation. Although there are very few such objects in our sample (see $N_2$ in Table 1), we have excluded them from our analysis since their anomalous colours could distort the global statistics. Most of these excluded objects are likely to be non-members, but it is possible that a fraction of the bluer objects are members that have recently undergone strong star formation. However, these excluded objects only account for a very small fraction (i.e. 5 %) of the total stellar mass in the early-type galaxies in our six sub-sample clusters (estimated from the $K$-band luminosity), hence they will not affect our analysis of the bulk of the stellar population. The remainder of the galaxies are represented with filled circles. Photometric random errors are shown only for 3C 324. All the other clusters have negligibly small errors, smaller than the size of the symbols.

We calculate the *C-M* regression lines using the BCES (bivariate, correlate errors and scatter) method of Akritas & Bershady (1996), who have kindly provided us with their software. Their program gives both the regression lines and the fitting errors analytically, considering the errors in both the magnitudes and the colours, as well as the intrinsic scatter of the data. The covariant errors are assumed to be equal to the errors in the magnitudes since the magnitude errors dominate the errors in the colours. Because the program considers the intrinsic scatter of the data, the error estimations of the fitting parameters are reliable; otherwise the fitting errors would be greatly underestimated. The regression line fits to the data are illustrated with the dashed lines in each of the *C-M* diagrams of Fig. 1.

The parameter fits are summarized in Table 1, where '$A$' is the zero-point colour of the regression line at the absolute magnitude $M_0$, and '$B$' is the slope of the line in $\Delta$(colour)/$\Delta$(mag) as,

$$(\mathrm{colour}) = A + B(\mathrm{mag} - M_0),$$

where mag and $M_0$ are absolute magnitudes. The regression lines for the three clusters from E97 (Cl 0016+16, Cl 0054−27 and Cl 0412−65) on the $V_{555}-I_{814}$ vs. $I_{814}^T$ plane, defined for spheroidal galaxies with apparent $I_{814}^T$ magnitudes brighter than 23 mag, are taken from their paper with the zero-points colours transformed to those at the absolute magnitude $I_{814}^T=-23$. The slopes and zero-points of the *C-M* relations for the SED98 sample have been taken from their paper as well. We adopted their $V-K$ colours for 8 clusters between $z=0.461$ and $0.689$, and $R-K$ colours for 3 clusters beyond that redshift, all of which are referred as $blue-K$ colours in their paper. Since they do not give the absolute colours of the *C-M* relation, we estimate the zero-points at $M_0$ from the absolute colours of their no-evolution *C-M* relation at $M_0$ and the average colour difference from it, both of which are given in the figures in SED98. We note that the errors in zero-point '$A$' in Table 1 include only the random errors of the data; the systematic errors of the photometry are not included, except for the SED98 sample. We discuss the systematic errors further in Sect. 4.2.

For the most distant cluster CIG J$0848+4453$ at $z=$1.273, we adopt $R-K$ colours and $K$ magnitudes of the six spectroscopically-confirmed cluster members for supplemental use, although morphology is unknown (Stanford et al. 1997). The *C-M* relation, however, cannot be defined due to the paucity of the number of galaxies. Thus, we measure the average colour and the standard deviation of the colours using the error of each colour as a weight, and regard these results as the zero-point colour and its error. These numbers are also listed in Table 1.

## 3. Model

### *3.1. Evolution of the colour-magnitude relation*

The elliptical galaxy models we have used are essentially the same as those built by KA97 (see also Kodama 1997 for details). Following Larson (1974) and Arimoto & Yoshii (1987), we assume elliptical galaxy formation occurs in a monolithic collapse accompanied by a galactic wind. Star formation is burst-like with very short star-formation and gas-infall time-scales (both are set to be 0.1 Gyr) followed by a galactic wind which occurs less than 0.5 Gyr from the start of galaxy formation. Chemical evolution is taken into account consistently under a well-mixed approximation. The model is calibrated to the *C-M* relation of Coma in the $V-K$ v.s. $M_V$ plane (BLE92) at $z=0$, either by changing the mean stellar metallicity (*metallicity sequence*) or the age (*age sequence)* of the galaxies.

We summarize now the small changes made on the KA97 models. The cosmological parameter $q_0$ was changed from the value $0.1$ used in KA97 to $0.5$. Following this change, we reconstructed the elliptical galaxy models to have an age 12 Gyr instead of 15 Gyr to be consistent with the shortening of the age of the Universe. In this cosmology ($q_0=0.5$), the lookback time of 12 Gyr corresponds to redshift $z\sim4.5$ (a lookback time of 15 Gyr corresponds to $z\sim5.4$ with $q_0=0.1$). In this paper, we also consider the metallicity sequence models for ages down to 9 Gyr ($z_f=1.2$). Another small difference is a change in the initial mass function slope. Hereafter, we use $x=1.10$ instead of the value $x=1.20$ adopted in KA97. The reason is the following. To construct the metallicity sequence model for

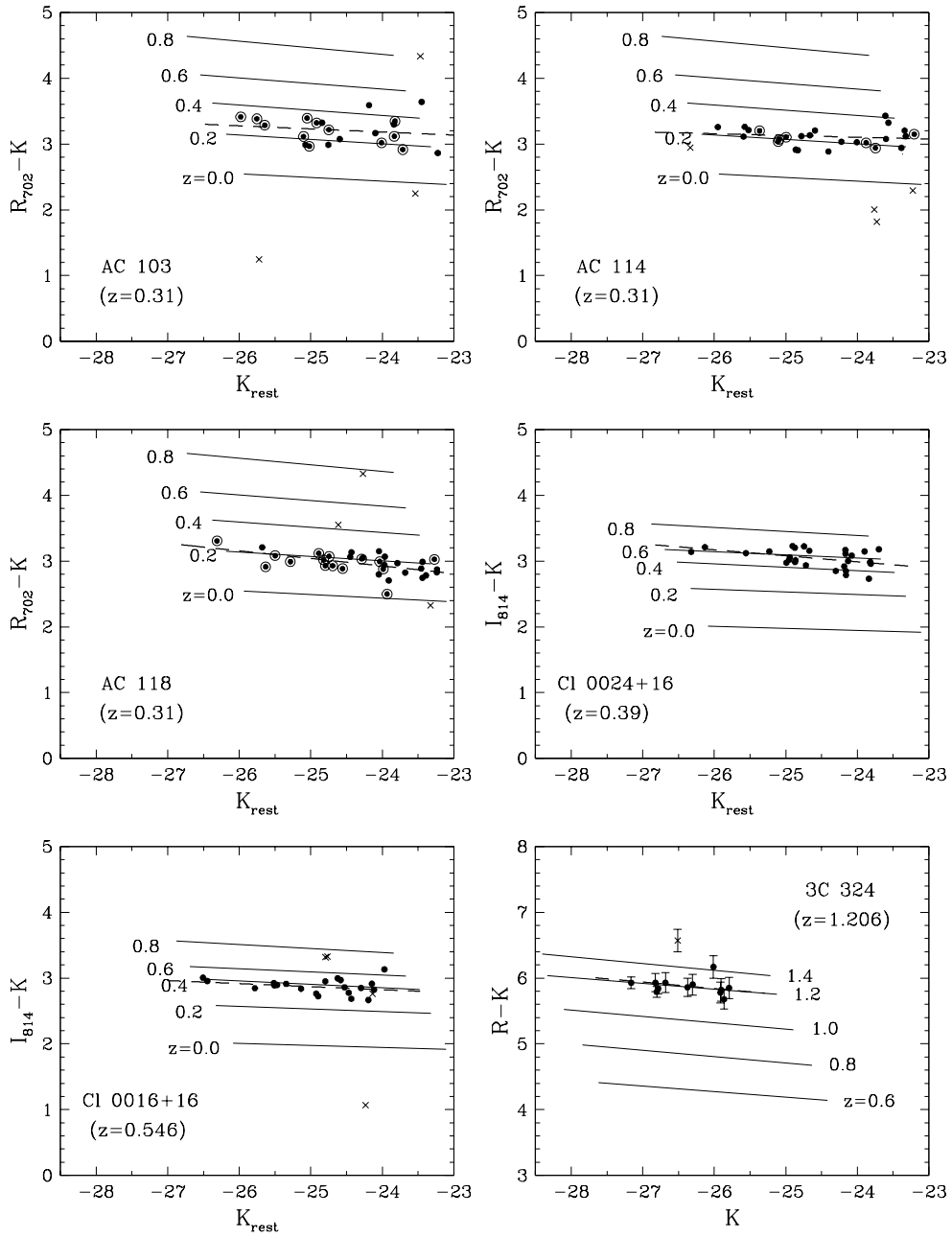


**Fig. 1.** *C-M* diagrams for the spheroidal galaxies in 6 of the clusters in our sample. Filled circles represent the spheroidal population in each cluster. An open circle surrounding a filled dot represents a spectroscopically confirmed cluster member. A cross indicates an apparent non-member, which we have excluded from our analysis. The dashed lines show the *C-M* relations as defined in the text. The solid lines show the model with $T_G = 12$ Gyr ($z_f \simeq 4.5$). The redshifts of the models increase from bottom to top, as indicated.

relatively younger ages, such as $9 - 10$ Gyr, the chemical yield is insufficient for $x = 1.20$, since the younger age population needs to be made up of higher metallicity material to reproduce the same colours. However, the analysis is almost totally independent of these small changes (KA97). The properties of the metallicity sequence of elliptical galaxies are summarized in Table 2, where $M_V$, $M_G$, $T_G$, $t_{gw}$, $Z_g(t_{gw})$, and $M/L_B$ are total absolute magnitude in $V$-band, total stellar mass, galactic age, time of the galactic wind, metallicity of the galactic gas at $t_{gw}$, and mass-to-light ratio in $B$-band of the model galaxies at $z = 0$, respectively. The luminosity-weighted mean stellar metallicities are given by two definitions; $\langle \log Z/Z_\odot \rangle$ and $\log\langle Z/Z_\odot \rangle$ (see KA97). The comparison with Coma ellipticals (BLE92) are presented in Fig. 2. Finally, we apply an aperture correction to the model when necessary, as described in Sect. 3.2.

We have simulated the evolution of the *C-M* relation as a function of redshift both in the observer's frame and in the rest frame for various photometric systems. The response curves are taken from Bessell (1990) for the Johnson $V$ and the Cousins $R$ and $I$ bands, and from Bessell & Brett (1988) for the $K$ band. The *HST* filter response functions for $V_{555}$, $R_{702}$, and $I_{814}$ are taken from the Space Telescope Science Institute web page. The photometric zero-points of the HST bands are taken from Holtzman et al. (1995).

To make a precise comparison with the data, the slope of the *C-M* relation at a given redshift is defined in the brightest 3 mag range of the model *C-M* relation by drawing a straight

**Table 2.** Model sequence of elliptical galaxies at $z = 0$ ($T_G$ =12 Gyr).

| | | | | | | | | |
|---|---|---|---|---|---|---|---|---|
| | $M_V$(mag) | −23.00 | −22.00 | −21.00 | −20.00 | −19.00 | −18.00 | −17.00 |
| | $M_G(10^9 M_\odot)$ | 848 | 311 | 115 | 42.4 | 15.7 | 5.85 | 2.18 |
| | $T_G$(Gyr) | 12.00 | 12.00 | 12.00 | 12.00 | 12.00 | 12.00 | 12.00 |
| | $t_{gw}$(Gyr) | 0.353 | 0.256 | 0.199 | 0.158 | 0.128 | 0.106 | 0.089 |
| *metallicity* | $\langle \log Z/Z_\odot \rangle$ | 0.061 | −0.038 | −0.132 | −0.229 | −0.328 | −0.425 | −0.523 |
| *sequence* | $\log\langle Z/Z_\odot \rangle$ | 0.202 | 0.094 | −0.005 | −0.101 | −0.196 | −0.290 | −0.382 |
| | $Z_g(t_{gw})$ | 0.566 | 0.417 | 0.298 | 0.188 | 0.084 | −0.010 | −0.099 |
| | $M/L_B$ | 8.830 | 8.002 | 7.113 | 6.459 | 5.978 | 5.451 | 5.049 |
| | $U-V$ | 1.668 | 1.591 | 1.516 | 1.440 | 1.365 | 1.295 | 1.228 |
| | $V-K$ | 3.355 | 3.274 | 3.194 | 3.113 | 3.033 | 2.952 | 2.871 |

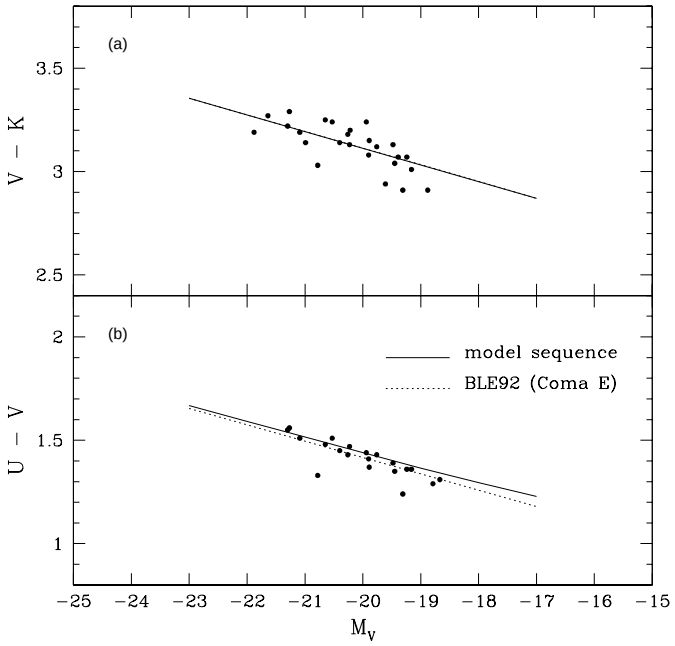


**Fig. 2a and b.** The *C-M* relation for Coma ellipticals. The filled circles represent the Coma ellipticals from Bower et al. (1992). The solid lines represent the loci of the metallicity sequence model with age 12 Gyr.

line between the two model galaxies which have $M_V^T = -23$ and $M_V^T = -20$ at $z = 0$, respectively, which is comparable to the definition of the slope for the observational data. Note that the *C-M* relation for the metallicity sequence is well represented by a straight line within the redshift range under consideration, and the above definition is quite reasonable. The zero-point of the model *C-M* relation is also defined at the absolute magnitude $M_0$, just as was done for the observational data.

The full tables of the evolution of the colours of elliptical galaxies in various combinations of age and metallicity and in various photometric systems will be presented in a separate paper in the supplement series (Kodama & Arimoto 1997, in preparation). The machine readable version of the tables will also be provided upon request.

### *3.2. Aperture correction*

Since early-type galaxies usually have radial colour gradients (e.g. Vader et al. 1988; Franx & Illingworth 1990; Peletier et al. 1990a; Peletier, Valentijn, & Jameson 1990b; Balcells & Peletier 1994), their colour indices will depend on the adopted aperture within which the galaxy light is integrated. Barger et al. (1996, 1997) used 5 arcsec aperture diameters to define their colour indices, which correspond to $\sim 14h^{-1}$ kpc for $z = 0.31$ and $\sim 18h^{-1}$ kpc for $z = 0.5$. On the other hand, BLE92 used 11 arcsec apertures for their Coma cluster galaxies, which corresponds to $5h^{-1}$ kpc. Since our model for elliptical galaxies is calibrated to match the *C-M* relation of the Coma ellipticals in BLE92, we need to take into account the aperture differences in order to accurately compare the models with the observational data.

We apply the aperture correction to the models instead of to the observational data of each cluster by constructing an aperture corrected *C-M* relation of Coma and recalibrating the model to match it (see KA97 for details). We adopt the value $\Delta(V-K)/(\log r/r_e) = -0.16$ given by Peletier et al. (1990b) as a typical bright elliptical galaxy colour gradient, where $r_e$ is the effective radius of the galaxy. González & Gorgas (1996) recently suggested that elliptical galaxies with stronger central $Mg_2$ indices show steeper line-strength gradients. If we consider the fact that the central $Mg_2$ strength strongly correlates with the velocity dispersion of the galaxy (Bender, Burstein, & Faber 1993; Jørgensen, Franx, & Kjærgaard 1996), then smaller ellipticals could have shallower colour gradients. However, González & Gorgas (1996) failed to detect significant correlations of the gradients with either absolute magnitude or galaxy mass, thus we have adopted a constant colour gradient for all galaxy models. We use the $M_K$ v.s. $\log r_e$ relation derived from the Kormendy relation of Pahre, Djorgovski, & Carvalho (1995) to apply aperture corrections to the various galaxy sizes. Using the colour gradient and the above relation, as well as the de Vaucouleurs (1948) $r^{1/4}$-law for the radial profile of ellipticals, we can reconstruct the standard *C-M* relation at $z = 0$ in the $V-K$ v.s. $M_V$ diagram for any given aperture using the BLE92 *C-M* relation for Coma.

The corrected *C-M* relations for Coma ellipticals are shown in Fig. 3 for three different physical aperture diameters, 28, 36, and 50 kpc. The first two correspond to 5 arcsec at $z = 0.31$

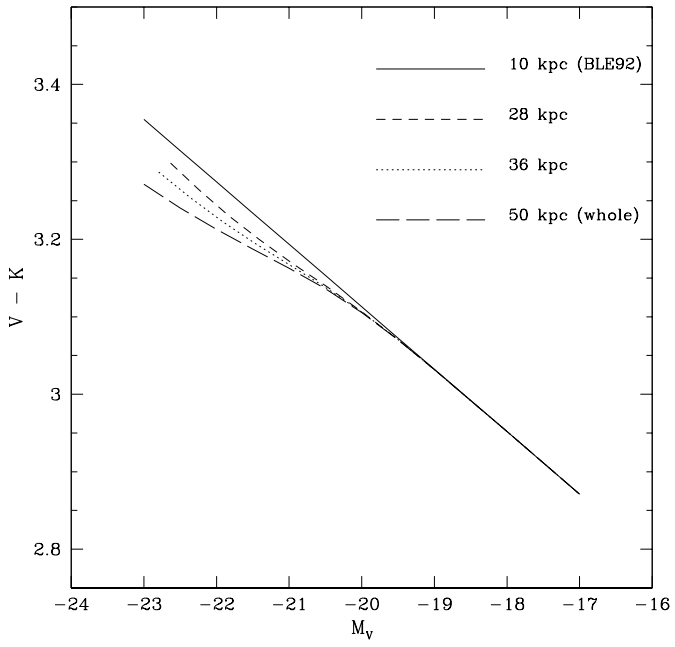


**Fig. 3.** Aperture corrected *C-M* relations for Coma ellipticals. Three *C-M* relations for different apertures are constructed from the Bower et al. (1992) relation for Coma ellipticals, taking into account the aperture correction ($h = 0.5$). The Bower et al. (1992) standard *C-M* relation is also shown.

and at $z = 0.5$, respectively ($h = 0.5$), while the third represents the relation for the whole galaxy. The *C-M* relation of BLE92 is indicated by the solid line. A bluing in the corrected *C-M* relation compared to that of BLE92 is observed for bright galaxies ($M_V \lesssim -20$ mag). This is because a larger aperture covers more of the physical size of the galaxy, which contains more blue light of presumably metal-poor stars. On the contrary, fainter galaxies have smaller physical sizes, and hence a 10 kpc aperture already covers most of the light of the galaxy and needs little correction. In spite of the bluing of the *C-M* relations, the changes in the slope for 28 and 36 kpc apertures are tempered. This is simply because the brighter galaxies lose more light outside the restricted aperture. The amount of dimming compared to the total magnitudes $M_V$ in BLE92 is larger for brighter galaxies. Thus, the aperture effect on the slopes of the *C-M* relation is kept rather small. For any redshift under consideration, the slope typically changes by only 0.01 and 0.02 per mag for the 28 kpc and 36 kpc apertures compared to the 10 kpc aperture, respectively. The effect on the zero-points of the *C-M* relation is negligibly small in any case (less than 0.05 mag).

When we compare the model to the photometric data for a given physical aperture, we regard the reconstructed *C-M* relation for Coma as the new standard relation, and the galaxy models are recalibrated so as to reproduce it at $z = 0$. The adopted aperture for the correction of the models are 28 kpc for AC 103, AC 114, and AC 118, and 36 kpc for Cl 0024+16, and Cl 0016+16. The $V_{555} - I_{814}$ colours for the three clusters from E97 have the same 10 kpc aperture as that of BLE92, and hence no correction is applied. For the rest of the clusters, including those from SED98, 3C 324, and CIG J0848+4453, the 28 kpc aperture model is applied, even though the SED98 sample and CIG J0848+4453 actually have $20-27$ kpc and 17 kpc diameter apertures, respectively. Here the apertures for SED98 clusters are provided from S.A. Stanford (private communication). This small aperture mismatch is negligible both in the slopes and in the zero-points. Note that the SED98 $K$ magnitudes are total magnitudes and not magnitudes inside 28 kpc, hence we apply a slight correction to the 28 kpc aperture model. Since we lack aperture information on the 3C 324 data, we adopt the 28 kpc aperture model arbitrarily. The corrections in the slope and zero-point are likely to be small when compared to the observational uncertainties.

## 4. Comparison

The model predictions for the evolution of the *C-M* relation are indicated by solid lines with changing redshift in Fig. 1 for the 6 clusters for which new *C-M* regression lines were determined in this work. The model is a metallicity sequence with an age of 12 Gyr ($z_f = 4.5$). As is evident from the figures, the observed *C-M* relations (dashed lines) are well defined in clusters up to $z \simeq 1.2$, and the slopes evolve almost in parallel, in good agreement with the model. The zero-points of the *C-M* relation for some of the clusters in Barger et al. (1997) deviate from the model prediction by as much as 0.2 mag. This probably arises from the zero-point uncertainties of the data. We discuss the zero-points in Sect. 4.2. The slopes of the model *C-M* relations seem to globally match the observed data very well. This strongly suggests that there is no differential evolution as a function of galaxy mass and that spheroidal galaxies in clusters form universally at high redshift. A detailed comparison with the models for these and the other clusters are given below.

### *4.1. Slopes*

The evolution of the slope of the *C-M* relation contains critical information on the origin of the *C-M* relation itself, i.e., which is the dominant factor controlling the systematic difference in the photometric properties as a function of galaxy luminosity. The evolution of the slope of the theoretical *C-M* relation is compared with the observed data in Fig. 4. The solid lines show the standard metallicity sequence model with $T_G = 12$ Gyr ($z_f \simeq 4.5$), the same as in Fig. 1. Almost all of the clusters are consistent with the model prediction of this single metallicity sequence with old age within $1.5\sigma$ errors. As is already mentioned in KA97, the metallicity sequence with an old age keeps the slope of the *C-M* relation essentially unchanged, although a slight steepening of the slope can be seen. The dotted lines indicate the no-evolution models estimated by simply redshifting the $z = 0$ models. The no-evolution models also show a slight steepening of the slope and are very close to the prediction of the $z_f \simeq 4.5$ metallicity sequence. This indicates that the steepening is simply due to the shift of corresponding wavelength shortwards with redshift. On the contrary, the dot-dashed lines correspond to the age sequence model; i.e., the ages become

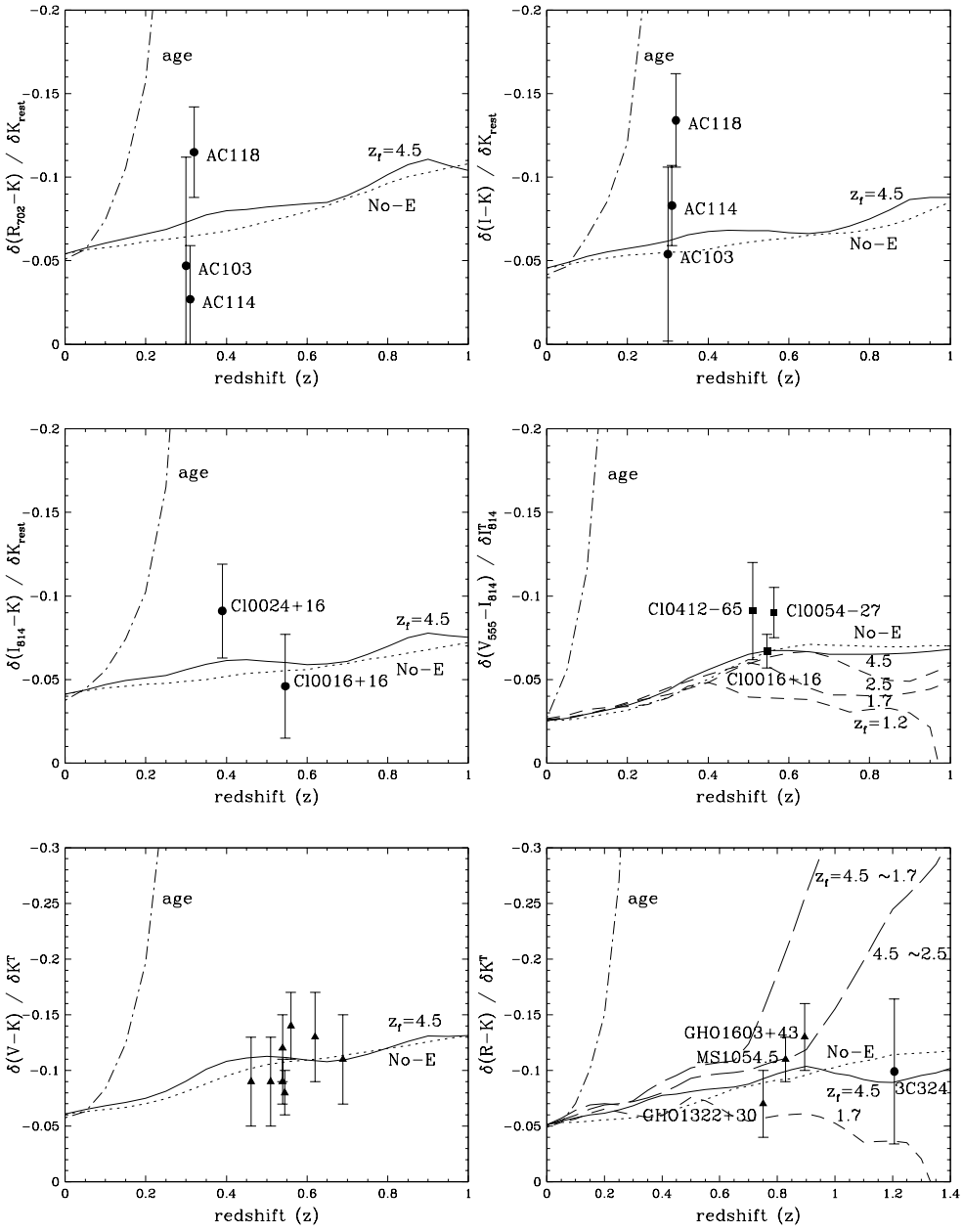


**Fig. 4.** Evolution of the slope of the *C-M* relation. The solid lines represent the metallicity sequence model with $z_f \simeq 4.5$ ($T_G = 12$ Gyr). The dashed lines correspond to models with different $z_f$s, as indicated in the figure. The long-dashed lines show the models that change $z_f$ as a function of galaxy luminosity for the brightest 3 mag range (brighter galaxies have larger values of $z_f$). The dash-dot lines show the extreme age sequence models from KA97. The dotted lines represent the no-evolution prediction (No-E). Our original results from the Barger et al. (1997) sample are shown by filled circles. The E97 and SED98 samples are indicated by filled squares and filled triangles, respectively. In the bottom-left panel, each observational point corresponds respectively to following cluster in ascending redshift order: 3C 295, Cl $0412-65$, GHO $1601+4253$ (down), MS $0451.6-0306$ (up), Cl $0016+16$, Cl $0054-27$, 3C 220.1, and 3C 34.

younger toward fainter galaxies along the *C-M* relation. As is evident, the pure age sequence is again absolutely rejected by all the clusters, which strengthens the conclusion of KA97.

Note that only AC 118 could have a somewhat steeper slope than the metallicity sequence model both in $R_{702}-K$ and $I-K$ (at the $1.5\sigma$ and $2\sigma$ levels, respectively), although still far away from the age sequence. The significance of the difference is too small to deserve further speculation. In fact, SED98 also measured the *C-M* slope for this cluster in a shorter wavelength colour ($G-K$, where $G$ denotes Gunn's $g$ filter) and found that it does not have a significantly steeper slope than the no-evolution Coma model.

Since one of our goals is to constrain the formation epoch from the *C-M* slope alone, we consider the younger metallicity sequence models as well. In the centre right panel of Fig. 4, we show three metallicity sequences with younger ages: $T_G = 11$ Gyr, $T_G = 10$ Gyr and $T_G = 9$ Gyr at $z = 0$, corresponding to $z_f \simeq 2.5$, 1.7, and 1.2, respectively. In the bottom right panel we also show the $z_f = 1.7$ model. The above models have been recalibrated to reproduce the Coma *C-M* relation at the fixed age by adjusting the mean stellar metallicity along the *C-M* relation. However, a strong constraint on the formation epoch cannot be made due to the large uncertainties in the slope, which is defined for only 3 mag from the brightest end of the *C-M* relation. Even the model with $z_f = 1.7$ cannot be rejected for many clusters. In Sect. 4.2 we show that the analysis of the zero-points is much more effective in providing direct information on the average formation epoch of the galaxies than that of the slopes.

However, the evolution of the *C-M* slope provides information on *relative* age variations of the early-type galaxies with

different luminosities. Thus we can constrain the maximum allowed age difference along the *C-M* relation. To do so, we introduce now a model in which age is differentially changed as a function of galaxy luminosity. The two long-dashed lines in the bottom right panel of Fig. 4 represent models which allow an age difference of 1 Gyr ($z_f = 4.5$–$2.5$) or 2 Gyr ($z_f = 4.5$–$1.7$) in the 3 mag range of the *C-M* relation with the brightest galaxies having the oldest age ($z_f = 4.5$). Note that the difference is much smaller than for the age sequence, which requires a $\sim 7$ Gyr difference. Despite the large uncertainties in the measured slopes, the four most distant clusters can clearly reject a 2 Gyr age difference, since the expected slopes at high redshift would be far too steep. If our models are correct, the age difference is unlikely to be more than 1 Gyr, and could be much smaller.

Our analysis of the evolution of the *C-M* slope indicates that there is little differential evolution in early-type galaxies as a function of galaxy luminosity, which strongly suggests that the bulk of the stars in early-type galaxies in rich cluster environments are coeval and form at a redshift well beyond unity. Moreover, we find little difference between the *C-M* slopes of different clusters, most of which are consistent with a universal metallicity sequence with old age. This argues for a universal mechanism responsible for the *C-M* relation of the early-type galaxies in these clusters. Their photometric properties may be described primarily by only one parameter: the mean stellar metallicity controlled by their mass.

### *4.2. Zero-points*

The zero-points of the *C-M* relation contain direct information on when the bulk of the stars formed in cluster early-type galaxies. In Fig. 5, the zero-points '$A$' of the *C-M* relation are compared with the models having various formation epochs. The zero-points from Barger et al. (1997) are not shown because of possible large uncertainties. The dotted line indicates the no-evolution model described above, and the four dashed lines correspond to the metallicity sequence models with $T_G$ =12, 11, 10, and 9 Gyr ($z_f = 4.5$, 2.5, 1.6, and 1.2), from top to bottom, respectively. In the comparison, the systematic errors of the photometry are also considered together with the random errors of the zero-points shown in Table 1. In E97 $0.04$ mag was given as the systematic error. For 3C 324, we conservatively choose 0.1 mag for the systematic errors. These numbers are added to the zero-point uncertainties of '$A$' which only take into account random errors. The systematic error on the zero-points of the SED98 clusters are estimated by the authors and are already included. Note again that the zero-point error of CIG J$0848+4453$ is the standard deviation of the galaxy colours.

At redshifts below 0.6, the differences in the zero-points for the model *C-M* sequences are too small to provide significant constraints on the formation epoch. Nevertheless, we can at least say that the zero-points of these clusters are well below the no-evolution prediction and are fully consistent with the metallicity sequence models with old age. Above that redshift, however, the zero-points get progressively more sensitive to the differences in formation epoch, as expected. Between $z$ =0.6 and 1.0, thanks to the small errors on the zero-points, the formation epoch of early-type galaxies in SED98's 5 clusters can be constrained to $z_f > 2$. Beyond $z = 1.0$, even a $0.2 - 0.3$ mag error is still small enough to discriminate between a 1 Gyr difference in galaxy age. In fact, as shown in the bottom left panel of Fig. 5, the early-type galaxies in the two most distant clusters 3C 324 and CIG J$0848 + 4453$ should have a high formation epoch, $z_f > 3$.

For $z > 1$ the predicted colours depend slightly on the adopted cosmology. The bottom right panel in Fig. 5 shows alternative cosmology models with $H_0 = 65$ km s$^{-1}$ Mpc$^{-1}$ and $q_0 = 0.05$. Each observational zero-point has been adjusted consistently with this cosmology due to a small shift of the position on the *C-M* line that corresponds to $M_K = -26$ mag, where the zero-point is defined, due to the change of distance modulus. Note that this correction is small, 0.02 mag or less. Although the latter cosmology gives redder model colours and the constraint on the formation epoch is slightly tempered, we can still say that the formation epoch should be above redshift 2. Even if the model uncertainties were as large as 0.2 magnitudes, the result would not be changed significantly. The bulk of the stars in early-type galaxies in cluster environments has to be formed at $z > 2$ even for this cosmology.

## 5. Discussion and conclusions

We have shown that the *C-M* relations of early type galaxies in clusters with $0.31 < z < 1.27$ have slopes consistent with passively evolving ellipticals of old age, with little differential evolution as a function of galaxy luminosity. The universality of the *C-M* slope at high $z$ is in good agreement with the results found for 45 lower redshift clusters ($0.02 < z < 0.18$) by López-Cruz (1997), suggesting that such universality is preserved over substantial look-back-times. Our model is fully consistent with the observed slopes in the *C-M* diagram for almost all of the clusters within one sigma errors (Kodama 1997). The zero-points of the *C-M* relation of high redshift clusters put strong constraints on the formation redshift of the bulk of the stars in cluster early-type galaxies: $z_f \geq 2 - 4$.

The following formation picture of cluster early-type galaxies, especially the ellipticals, arises from our analysis: Their stars are, on the whole, very old, and the galaxies follow a universal function of galaxy mass. The differences along the *C-M* sequence are governed by the mean stellar metallicity. Most of the early-type galaxies in rich clusters form very quickly and effectively in the deep potential well of the clusters at significantly high redshift, and galactic wind feedback probably plays a key role in producing the *C-M* relation. Since elliptical galaxies are major constituents in the core regions of galaxy clusters, the present study strongly suggests that the central region of these clusters formed almost at the same time in the early universe and by the same mechanism.

As shown in Fig. 5, the zero-point analysis of the *C-M* relation provides very high sensitivity to the formation epoch of the galaxies for clusters with $z > 1$ even with moderately accu-

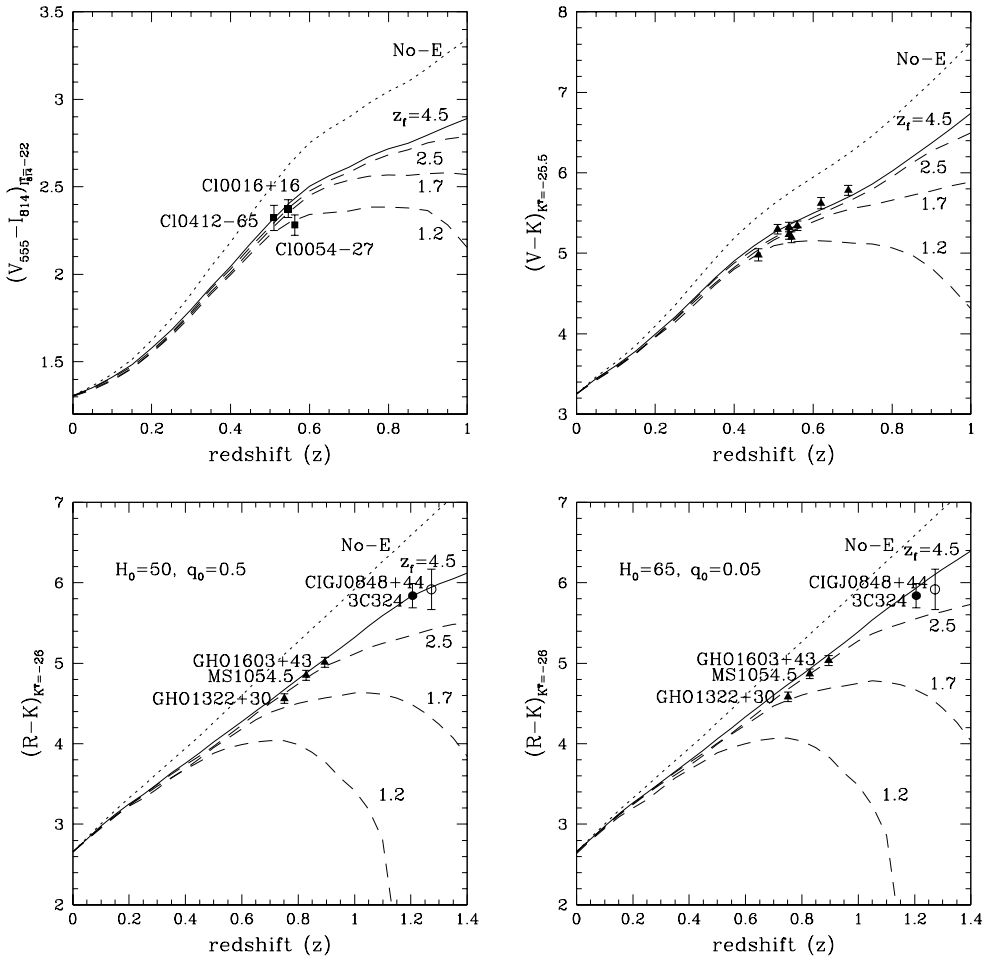


**Fig. 5.** Evolution of the zero-point of the *C-M* relation. The dotted line indicates the no-evolution model (No-E). The solid lines represent the metallicity sequence model with $z_f \simeq 4.5$ ($T_G = 12$ Gyr). The dashed lines correspond to $z_f \simeq$ 2.5, 1.6, and 1.2, ($T_G$ =11, 10, and 9 Gyr) from top to bottom, respectively. The observed data are shown by the symbols used in Fig. 4. The average and the standard deviation of the galaxy colours in CIG J0848+44 ($z$ =1.273) are also shown by an open circle and an error bar. In the top-right panel, each observational point corresponds respectively to following cluster in ascending redshift order: 3C 295, Cl $0412-65$, GHO $1601+4253$ (up), MS $0451.6-0306$ (down), Cl $0016+16$, Cl $0054-27$, 3C 220.1, and 3C 34.

rate photometry (errors$\sim 0.1$ mag). Differences of $\sim 1$ Gyr are easily measurable at such high redshifts. Therefore, photometry of early-type galaxies in clusters beyond $z \sim 1$ can accurately determine the formation epoch of these galaxies. Furthermore, the slope of the *C-M* relation at redshifts beyond $z \sim 1$ is so sensitive to age difference (as suggested by the long-dashed lines in the bottom right panel of Fig. 4) that it will allow us to investigate systematic difference of mean stellar age as small as $\simeq$1 Gyr as a function of galactic mass, if they are present. We expect slope changes to be especially prominent when we approach the star formation phase of the elliptical galaxies.

We have not discussed the colour scatter around the *C-M* relation in this paper, but SED98 pointed out that the scatter dose not increase with redshift out to $z \sim 1$. It would be extremely important to determine when the *C-M* relation breaks down: i.e. when its scatter becomes very large. This would indicate the very time when the ellipticals are forming.

Unfortunately, only a handfull of clusters have been found beyond $z \sim 1$. Searching for such distant clusters and pushing the *C-M* relation analysis towards higher redshifts must be a promising strategy to determine the formation epoch of cluster ellipticals globally and as a function of their mass. The advent of large format near-infrared arrays provides the means to carry out that search efficiently.

We finish with a word of caution. Our study is based on the monolithic model for the formation of early-type galaxies. The data we have analyzed here is fully consistent with this model, but it might not be the only solution. In particular, an alternative scenario set in the context of the hierarchical merging model of galaxy formation (e.g. Kauffmann & Charlot 1997) could give results that are also broadly consistent with the available data, although it has not been fully confirmed yet. A detailed comparison of the observed properties of the *C-M* relation in distant clusters with the predictions of hierarchical models that properly take chemical evolution into account is clearly needed. It is especially important to test whether this type of model can give the universal *C-M* relation for different clusters locally and over a wide range of redshift, since merging histories are likely to have varied from cluster to cluster. Moreover it is not yet confirmed that larger ellipticals form always from larger spirals already enriched in metal. In any case, however, if we define the formation epoch of the early-type galaxies as the time when the bulk of their stars formed, the properties of the *C-M* relation place that epoch well beyond $z = 2$, independent of which formation picture is correct.

*Acknowledgements.* We thank R.S. Ellis, R.G. Bower and S.A. Stanford for discussions. We are grateful to S.A. Stanford for giving us continuous information of SED98 paper before publication. TK thanks

the Japan Society for Promotion of Science (JSPS) for financially supporting his stay at the Institue of Astronomy, Cambridge, UK. NA thanks the JSPS for supporting his stay in Observatoire de Paris. This work was financially supported in part by a Grant-in-Aid for the Scientific Research (No.09640311) by the Japanese Ministry of Education, Culture, Sports and Science. AAS acknowledges generous financial support from the Royal Society.

## References

Akritas, M. G., & Bershady, M. A., 1996, ApJ, 470, 706
Aragón-Salamanca, A., Ellis, R. S., Couch, W. J., & Carter, D., 1993, MNRAS, 262, 764
Arimoto, N., & Yoshii, Y., 1987, A&A 173, 23
Balcells, M., & Peletier, R. F., 1994, AJ, 107, 135
Barger, A. J., Aragón-Salamanca, A., Ellis et al., 1996, MNRAS, 279, 1
Barger, A. J., Aragón-Salamanca, A., Smail et al., 1997, ApJ, in press
Bender, R., Burstein, D., & Faber, S. M., 1993, ApJ, 411, 153
Bessell, M. S., & Brett, J. M., 1988, PASP, 100, 1134
Bessell, M. S., 1990, PASP, 102, 1181
Bower R. G., Lucey J. R., & Ellis R. S., 1992, MNRAS 254, 601 (BLE92)
Burstein, D., & Heiles, C., 1984, ApJS, 54, 33
Couch, W. J., Shanks, T., & Pence, W. D., 1985, MNRAS, 213, 215
Couch, W. J., Barger, A. J., Smail, I., Ellis, R. S., & Sharples, R. M., 1997, ApJ, in press
de Vaucouleurs, G., 1948, Ann. d'Astrophys., 11, 247
Dickinson, M., 1996, in: Fresh Views of Elliptical Galaxies, eds. A. Buzzoni, A. Renzini, & A. Serrano (ASP Conf. Ser. Vol. 86), p. 283
Dressler, A., Oemler, Jr., A., Couch, W. J. et al., 1997, ApJ, in press
Ellis, R. S., Couch, W. J., MacLaren, I., & Koo, D. C., 1985 ApJ, MNRAS, 217, 239
Ellis, R. S., Smail, I., Dressler et al., 1997, ApJ, 483, 582 (E97)
Franx, M., & Illingworth, G. D., 1990, ApJ, 359, L41
González, J. J., & Gorgas, J. 1996, in: Fresh Views of Elliptical Galaxies, ed. A., Buzzoni, A. Renzini, & A. Serrano (ASP Conf. Ser. Vol. 86), p. 225
Holtzman, J. A., Burrows, A. J., Casertano, S. et al., 1995, PASP, 107, 1065
Jørgensen, I., Franx, M., & Kjærgaard, P., 1996, MNRAS, 280, 167
Kauffmann, G., & Charlot, S., 1997, preprint, astro-ph/9704148
Kodama, T., 1997, Ph.D. Thesis, University of Tokyo
Kodama, T., Arimoto, N., 1997, A&A, 320, 41 (KA97)
Larson, R. B., 1974, MNRAS, 166, 585
López-Cruz, O., 1997, Ph.D. Thesis, University of Toronto
Pahre, M. A., Djorgovski, S. G., & de Carvalho, R. R., 1996, ApJ, 456, L79
Peletier, R. F., Davies, R. L., Illingworth, G. D., Davis, L. E., & Cawson, M., 1990a, AJ, 100, 1091
Peletier, R. F., Valentij,n, E. A., & Jameson, R. F., 1990b, A&A, 233, 62
Smail, I., Dressler, A., Couch, W. C. et al., 1997, ApJS, 110, 481
Stanford, S. A., Eisenhardt, P. R. M., & Dickinson, M., 1995, ApJ, 450, 512
Stanford, S. A., Eisenhardt, P. R. M., & Dickinson, M., 1998, ApJ, 492, 461 (SED98)
Stanford, S. A., Elston, R., Eisenhardt, P. R. M. et al., 1997, AJ, 114, 2232
Vader, J. P., Vigroux, L., Lachièze-Rey, M., & Souviron, J., 1988, A&A, 203, 217
Visvanathan, N., & Sandage, A., 1977, ApJ, 216, 214